

The Intrinsic Alignment of Dark Halo Substructures

JOUNGHUN LEE^{1,2}, XI KANG³, AND YIPENG JING³

ABSTRACT

We investigate the intrinsic alignments of dark halo substructures with their host halo major-axis orientations both analytically and numerically. Analytically, we derive the probability density distribution of the angles between the minor axes of the substructures and the major axes of their host halos from the physical principles, under the assumption that the substructure alignment on galaxy scale is a consequence of the tidal fields of the host halo gravitational potential. Numerically, we use a sample of four cluster-scale halos and their galaxy-scale substructures from recent high-resolution N-body simulations to measure the probability density distribution. We compare the numerical distribution with the analytic prediction, and find that the two results agree with each other very well. We conclude that our analytic model provides a quantitative physical explanation for the intrinsic alignment of dark halo substructures. We also discuss the possibility of discriminating our model from the anisotropic infall scenario by testing it against very large N-body simulations in the future.

Subject headings: cosmology:theory — large-scale structure of universe

1. INTRODUCTION

The dark halo substructure has recently come to one of the most lively topics in cosmology. Although the standard cosmological paradigm based on the cold dark matter (CDM) concept generically predicts the presence of the substructure inside the dark matter halos, there are many questions yet to be answered associated with the dark halo substructures. The intrinsic alignment effect of the dark halo substructure is one of those questions.

¹School of Physics, Korea Institute for Advanced Study, Seoul 207-43, Korea ;
jounghun@newton.kias.re.kr

²Astronomy Program, School of Earth and Environmental Sciences, Seoul National University, Seoul 151-742 , Korea

³Shanghai Astronomical Observatory; the Partner Group of MPA, Nandan Road 80, Shanghai 200030, China ; kangx@shao.ac.cn

There are plenty of observational evidences that the major axes of the brightest cluster galaxies (BCGs) have a strong tendency to be aligned with that of their host clusters (Sastry 1968; Carter & Metcalfe 1980; Binggeli 1982; Struble & Peebles 1985; Rhee & Katgert 1987; West 1989, 1994; Plionis 1994; Fuller, West & Bridges 1999; Kim et al. 2002). The most popular theory for the BCG alignment is the anisotropic infall scenario based on the standard hierarchical clustering model (West 1989): The initial density field of CDM is web-like, interconnected by the primordial filaments (Bond 1987; Bond, Kofman, & Pogosyan 1996). The gravitational collapse and merging to form structures occurs not in an isotropic way but in an anisotropic way along the large-scale filaments. Accordingly, the infall of materials into a cluster also occurs along the primordial filament, which will induce the alignment between the orientation of a host cluster and that of BCG embedded in it.

There are several reasons that the anisotropic infall theory became so popular: Being simple and intuitive, it fits very well into the cold dark matter paradigm. In addition, it has been supported by several numerical simulations (e.g., West, Villumsen, & Dekel 1991; van Haarlem & van de Weygaert 1993; Dubinski 1998; Faltenbacher et al. 2002) which demonstrated that the gravitational infall and merging of materials indeed occurs along the filaments.

Nevertheless, the theory is only qualitative and still incomplete. Recent observations indicate that not only the BCGs but also the less dominant cluster galaxies exhibit the alignment effect to a non-negligible degree (Plionis & Basilakos 2002; Plionis et al. 2003; Pereira & Kuhn 2004). In the anisotropic infall model, the substructure alignment is a primordial effect, and would get damped away quickly by the subsequent nonlinear processes such as the violent relaxation, the secondary infall, and so on (Quinn & Binney 1992; Coutts 1996). Therefore, it is very unlikely that the cluster galaxies other than the BCGs keep the primordial alignment effect till the present epoch (Plionis et al. 2003). Here, we propose that the initial tidal interaction between the subhalos and the host halo will be responsible for the observed intrinsic alignment of the cluster galaxies.

2. ANALYTICAL PREDICTIONS

When a subhalo forms inside a host halo, it acquires the angular momentum $\mathbf{L} = (L_i)$ due to the tidal shear field $\mathbf{T} = (T_{ij})$ generated by the gravitational potential of the host halo (Ψ): $T_{ij} \equiv \partial_i \partial_j \Psi$. Lee & Pen (2000, 2001) proposed the following formula to quantify the mutual correlations between \mathbf{T} and \mathbf{L} :

$$\langle L_i L_j | \hat{\mathbf{T}} \rangle = \frac{1+c}{3} \delta_{ij} - c \hat{T}_{ik} \hat{T}_{kj}. \quad (1)$$

where $c \in [0, 1]$ is a correlation parameter to quantify the strength of the correlation between $\hat{\mathbf{T}}$ and \mathbf{L} , and $\hat{\mathbf{T}} = (\hat{T}_{ij})$ is a unit traceless tidal shear tensor defined as $\hat{T}_{ij} \equiv \tilde{T}_{ij}/|\tilde{\mathbf{T}}|$ with $\tilde{T}_{ij} \equiv T_{ij} - \text{Tr}(\mathbf{T})\delta_{ij}/3$, and $\mathbf{L} = (L_i)$ is a rescaled but not a unit angular momentum. If we replace the rescaled angular momentum by the unit angular momentum, $\hat{\mathbf{L}}_i \equiv \mathbf{L}/|\mathbf{L}|$ in equation (1), then the correlation parameter c is reduced by a factor of $3/5$. Note here that the LHS of equation (1) represents a *conditional* ensemble average of $L_i L_j$ provided that the unit traceless tidal shear tensor is given as \hat{T}_{ij} . For the detailed explanations of equation (1), see Appendix A in Lee & Pen (2001).

It is naturally expected that c decreases with time as the correlation between $\hat{\mathbf{T}}$ and \mathbf{L} must decrease after the moment of the turn-around due to the subsequent nonlinear process. Lee & Pen (2002) found $c \sim 0.3$ at present epoch by analyzing the data from the Tully Galaxy Catalog and the Point Source Redshift Catalog Redshift Survey (in their original work, they used a reduced correlation parameter $a \equiv 3c/5$ and found $a = 0.18$).

Strictly speaking, equation (1) holds only if $\hat{\mathbf{T}}$ and \mathbf{L} are defined at the same positions (Lee & Pen 2000, 2001). Here, they don't: $\hat{\mathbf{T}}$ and \mathbf{L} are defined at the centers of the mass of the host halo and the subhalo, respectively. For simplicity, here we just assume that equation (1) still holds, ignoring the separation between the centers of the mass of the subhalos and that of the host halo.

The distribution of \mathbf{L} under the influence of the tidal field is often regarded as Gaussian (Catelan & Theuns 1996; Lee & Pen 2001):

$$P(\mathbf{L}) = \frac{1}{[(2\pi)^3 \det(M)]^{1/2}} \exp \left[-\frac{L_i (M^{-1})_{ij} L_j}{2} \right], \quad (2)$$

where the covariance matrix $M_{ij} \equiv \langle L_i L_j | \hat{\mathbf{T}} \rangle$ is related to the tidal shear field $\hat{\mathbf{T}}$ by equation (1). In the principal axis frame of $\hat{\mathbf{T}}$, let us express \mathbf{L} in terms of the spherical coordinates: $\mathbf{L} = (L \sin \theta \cos \phi, L \sin \theta \sin \phi, L \cos \theta)$ where $L \equiv |\mathbf{L}|$, and θ and ϕ are the polar and the azimuthal angles of \mathbf{L} . Note that the polar angle θ represents the angle between the direction of \mathbf{L} of the subhalo and the minor principal axis of $\hat{\mathbf{T}}$ of its host.

The probability density distribution of the cosines of the polar angle θ can be obtained by integrating out equation (2) over L and ϕ (Lee 2004):

$$\begin{aligned} p(\cos \theta) &= \frac{1}{2\pi} \prod_{i=1}^3 \left(1 + c - 3c\hat{\lambda}_i^2 \right)^{-\frac{1}{2}} \times \\ &\quad \int_0^{2\pi} \left(\frac{\sin^2 \theta \cos^2 \phi}{1 + c - 3c\hat{\lambda}_1^2} + \frac{\sin^2 \theta \sin^2 \phi}{1 + c - 3c\hat{\lambda}_2^2} + \frac{\cos^2 \theta}{1 + c - 3c\hat{\lambda}_3^2} \right)^{-\frac{3}{2}} d\phi. \end{aligned} \quad (3)$$

Here the polar angle θ is forced to be in the range of $[0, \pi/2]$ satisfying $\int_0^{\pi/2} p(\theta) \sin \theta d\theta = 1$, since we care about the relative spatial orientation of the subhalo axis, but not its sign. Here the three $\hat{\lambda}_i$'s ($i = 1, 2, 3$) are the eigenvalues of $\hat{\mathbf{T}}$ in a decreasing order satisfying the following two conditions: (i) $\sum_i \hat{\lambda}_i = 0$; (ii) $\sum_i \hat{\lambda}_i^2 = 1$. If \mathbf{T} is a Gaussian random field which is true in the linear regime, one can show that $\hat{\lambda}_1 \approx -\hat{\lambda}_3 \approx 1/\sqrt{2}$ and $\hat{\lambda}_2 \approx 0$ (Lee & Pen 2001).

We adopt the following two assumptions: (i) On cluster scale, the principal axes of the inertia shape tensor I_{ij} of a host halo is aligned with its tidal shear tensor T_{ij} with the eigenvalues being in an opposite order. In other words, the major principal axis of I_{ij} is the minor principal axis of T_{ij} , and vice versa. Note that in Lee (2004), it was erroneously stated that it the major axis of I_{ij} is the major axis of T_{ij} (Trujillo, Carretero, & Juncosa 2004 in private communication); (ii) The minor axis of a subhalo is in the direction of its angular momentum.

A justification of the first assumption is given by the Zel'dovich approximation (Zel'dovich 1970) which predicts a perfect alignment between the principal axis of I_{ij} and that of T_{ij} . Since the cluster-size halos are believed to be in the quasi-linear regime where the Zel'dovich approximation is valid, the first assumption should provide a good approximation to the reality. Moreover, recent N-body simulations indeed demonstrated that I_{ij} and T_{ij} are quite strongly correlated (Lee & Pen 2000; Porciani, Dekel, & Hoffman 2002). Regarding the second assumption, there is an established theory that the spin axis of an ellipsoidal object in the gravitational tidal field is well correlated with its minor axis (Binney & Tremaine 1987), which was also confirmed by several N-body simulations (e.g., Faltenbacher et al. 2002)

Now that the minor principal axis of $\hat{\mathbf{T}}$ is the major axis of the host halo, and \mathbf{L} is aligned with the minor axis of the subhalo, the polar angle θ in equation (3) actually equals *the angle between the minor axis of the subhalo and the major axis of the host halo*. Putting $\hat{\lambda}_1 = 1/\sqrt{2}$, $\hat{\lambda}_2 = 0$, and $\hat{\lambda}_3 = -1/\sqrt{2}$, we simplify equation (3) into

$$p(\cos \theta) = \frac{1}{2\pi} (1+c) \sqrt{1 - \frac{c}{2}} \int_0^{2\pi} \left[1 + c \left(1 - \frac{3}{2} \sin^2 \theta \sin^2 \phi \right) \right]^{-3/2} d\phi, \quad (4)$$

In the asymptotic limit of $c \ll 1$, equation (4) can be further simplified into the following closed form:

$$p(\cos \theta) = \left(1 - \frac{3c}{4} \right) + \frac{9c}{8} \sin^2 \theta \quad (5)$$

Equations (4) and (5) imply that $p(\theta)$ increases as θ increases. That is, the minor axis of a subhalo has a strong propensity to be *anti-aligned* with the major axis of its host halo. Hence, it explains the observed alignment effect between the subhalo and the host halo major

axes as a consequence of the intrinsic anti-alignment between the subhalo minor axis and the host halo major axis.

The value of c in equations (4) and (5) should depend on the distance from the host halo center (r), the subhalo mass (m) and redshift (z): $c = c(r, m, z)$. What one can naturally expect is that c should decrease with r since the tidal interaction must be strongest in the inner part of the host halo, and that c should increase with m and r since the alignment effect gets reduced in the nonlinear regime. Unfortunately, it will be very difficult to find the functional form of $c(r, z, m)$ as c contains all the nonlinear informations of galaxy evolution. We do not attempt to find $c(r, z, m)$ here since it is beyond the scope of this Letter. Instead, we simply assume that c is a constant, and determine the value of c empirically by fitting equation (4) to the numerical results in §3.

3. NUMERICAL EVIDENCES

The data we use in this Letter is the high resolution halo simulations of Jing & Suto (2000). First they selected dark matter halos from their previous cosmological P³M N-body simulations with 256^3 particles in a $100h^{-1}\text{Mpc}$ cube (Jing & Suto 1998). The halos were identified using the standard friend-of-friend (FOF) algorithm, among which four halos on cluster-mass scales (with mass around $5 - 10 \times 10^{14}h^{-1}M_\odot$) were then re-simulated using the nested-grid P³M code which was designed to simulate high-resolution halos. The force resolution is typically 0.4% of the virial radius, and each halo is represented by about 2×10^6 particles within the virial radius. We then use the SUBFIND routine of Springel et al. (2001) to identify the disjoint self-bound subhalos within these halos, and include those subhalos containing more than 10 particles in the analysis. These simulations adopted the “concordance” Λ CDM cosmology with $\Omega_0 = 0.3$, $\Omega_{\Lambda,0} = 0.7$, and $h = 0.7$.

Using this numerical data, we first compute the inertia tensors as $I_{ij} \equiv \sum_\alpha m_\alpha x_{\alpha,i}x_{\alpha,j}$ for each host halo and its subhalos in their respective center-of-mass frames. Then, we find the directions of the eigenvectors corresponding to the largest and the smallest eigenvalues of the host halo and the subhalo inertia tensors, respectively, by rotating the inertia tensors into the principal axes frame, and determine the major axes of each host halo and the minor axis of its subhalos. Then, we measure the cosines of the angles, θ , between the major axis of the host halo and the minor axes of their subhalos by computing $\cos\theta \equiv \hat{\mathbf{e}}_h \cdot \hat{\mathbf{e}}_s$ where $\hat{\mathbf{e}}_h$ and $\hat{\mathbf{e}}_s$ represent the major and the minor axes of the host halo and its subhalos, respectively. Finally, we find the probability density distribution, $p(\cos\theta)$, by counting the number density of the subhalos. When computing the probability density distribution, we use all the subhalos in the host halo linked by the FOF algorithm.

We perform the above procedure at four different redshifts: $z = 0, 0.5, 1$ and 2 . The total number of the subhalos N_{tot} at each redshift is 8963, 5686, 2766, and 1469, respectively. Figure 1 plots the final numerical distributions (solid dots) with the error bars. The error bar at each bin is nothing but the Poisson mean for the case of no alignment given as given as $1/\sqrt{N_{bin} - 1}$ where N_{bin} is the number of the subhalos at each bin. As one can see, the numerical distribution $p(\cos \theta)$ increases as θ increases, revealing that the minor axes of substructures really tend to be anti-aligned with the major axes of their host halos, as predicted by the analytic model (eq.[4]) of §2. Figure 1 also plots the analytic predictions (solid line) and the approximation formula (dashed line) derived in §2. The horizontal dotted line represents the uniform distribution of $\cos \theta$ for the case of no alignment.

We fit the analytic distributions to the numerical data points to determine the best-fit values of the correlation parameter c . We find $c = 0.28 \pm 0.01, 0.36 \pm 0.02, 0.41 \pm 0.02, 0.45 \pm 0.03$ at $z = 0, 0.5, 1, 1.5$, respectively. The errors involved in the determination of c is given as the standard deviation of c for the case of no alignment effect given as $\epsilon_c \equiv \sqrt{c^2/(N_{tot} - 1)}$ where N_{tot} is the number of all subhalos used to compute c . The value of c increases with redshifts z , as expected.

In fact the value of $c = 0.3$ gives quite a good fit, if not the best, not only at the present epoch of $z = 0$ but also at all earlier epochs of $z = 0.5, 1, 1.5$, which implies that the initially induced anti-alignment effect is more or less conserved, reflecting the fact that the directions of the subhalo angular momentum are fairly well conserved.

To understand the dependence of the alignment effect on the subhalo mass, we derive the same probability distribution but by using only the most massive 30 subhalos in each cluster ($N_{tot} = 120$ for each redshift), and find the corresponding best-fit values of c . We find $c = 0.8 \pm 0.11, 0.85 \pm 0.11, 0.9 \pm 0.11, 0.95 \pm 0.11$ at $z = 0, 0.5, 1, 1.5$, respectively. Figure 2 plots the results. The approximation formula (eq.[5]) is excluded in this figure since the best-fit values of c for this case is pretty close to unity. Although the large error bars prevent us from making a quantitative statement, it is obvious that the anti-alignment effect is stronger for the case massive subhalos.

4. SUMMARY AND DISCUSSIONS

Although the currently popular anisotropic merging and infall scenario has provided a qualitative explanation for the BCG-cluster and cluster-cluster alignments (e.g., Hopkins, Bahcall & Bode 2005), no previous approach based on this scenario was capable of making a quantitative prediction for the alignment effect of cluster galaxies other than BCGs with

the host clusters. We constructed an analytic model where the substructure alignment is a consequence of the tidal field of the host halo at least on the scale of cluster galaxies, and predicted quantitatively the strength of the alignment effect, by comparing the model with the results from recent high-resolution N-body simulations.

However, it is worth noting that we have yet to completely rule out the anisotropic infall model. An idealistic way to discriminate our analytic model from the anisotropic infall scenario would be to measure directly the correlation of the directions of the subhalo angular momentum with the host halo orientations. Unfortunately, it is very difficult to determine the directions of the subhalo angular momentum vectors in current simulations. Because the rotation speed of a dark halo in simulations is only a few percent of the virial motion of the particles, one needs more than 10^4 particles to determine accurately the direction of the angular momentum vector of a subhalo with an average rotation speed. In current simulations the subhalos have much fewer particles than 10^4 . This is why we used the minor axes of the subhalos rather than the directions of the subhalo angular momentum vectors to investigate the intrinsic alignments of substructures.

Nevertheless, the strong alignment between the halo minor axes and angular momentum vectors (Binney & Tremaine 1987) should indicate indirectly that the anti-alignments between the subhalo minor axes and the host halo major axes observed in our simulations are likely to be caused by the host halo tidal field as our model predicts. Many N-body simulations (Barnes & Efstathiou 1987; Dubinski 1992; Warren et al. 1992; Bailin et al. 2005) have already proved that the dark matter halos rotate and their angular momentum vectors are aligned with their minor axes. Furthermore, Bailin & Steinmetz (2004) demonstrated evidently that there are good internal alignments between the halo minor axes and angular momentum vectors measured at different radii. Therefore, the alignments between the halo angular momentum vectors and the minor axes are expected to be hold even when the outer parts of the halos get disrupted when they fall into larger halos as substructures. Indeed, we ourselves check this effect in our simulations: we measure the angular momentum vectors of several very massive subhalos with more than 10^4 particles, and find that the subhalos have *non-zero* angular momentum and that the subhalo minor axes are strongly aligned the directions of their angular momentum: the cosines of all alignment angles turn out to be bigger than 0.6.

Anyway, it will be definitely necessary to investigate directly the correlations of the directions of the subhalo angular momentum with the orientations of their host halos in the future with larger simulation data, where the number of particles belonging to subhalos should be large enough. Using larger simulation data, it will be also possible to determine the functional form of the correlation parameter $c(r, m, z)$. Our future work is in this direction.

We thank the anonymous referee who helped us improve the original manuscript. J.L. wishes to thank the Shanghai Astronomical Observatory for a warm hospitality during the workshop on Cosmology and Galaxy Formation where this collaboration began. J.L. is supported by the research grant of the Korea Institute for Advanced Study. X.K. and Y.P.J. are partly supported by NKBRSP (G19990754), by NSFC(Nos. 10125314, 10373012), and by Shanghai Key Projects in Basic Research (No. 04jc14079)

REFERENCES

Adams, M. T., Strom, K. M., & Strom, S. F. 1980, *ApJ*, 238, 445

Bailin, J., & Steinmetz, M. 2004, *ApJ*, in press, (astro-ph/0408163)

Bailin, J. et al. 2005, *ApJ*, in press, astro-ph/0505523

Bardeen, J. M., Bond, J. R., Kaiser, N., & Szalay, A. S. 1986, *ApJ*, 304, 15

Barnes, J., & Efstathiou, G. 1987, *ApJ*, 319, 575

Binggeli, B. 1982, *A&A*, 107, 338

Binney, J., & Tremaine, S. 1987, *Galactic Dynamics*, (Princeton: Princeton Univ. Press)

Binggeli, B. 1982, *A&A*, 107, 338

Bond, J. R. 1987, in *Nearly Normal Galaxies*, ed. S. Faber (New York: Springer), 388

Bond, J., R., Kofman, L., & Pogosyan, D. 1996, *Nature*, 380, 603

Carter, D., & Metcalfe, J. 1980, *MNRAS*, 191, 325

Catelan, P., & Theuns, T. 1996, *MNRAS*, 282, 436

Coutts, A. 1996, *MNRAS*, 278, 87

Dubinski, J. 1992, 401, 441

Dubinski, J. 1998, 502, 141

Faltenbacher, A., Kerscher, M., Gottloeber, S., & Mueller, M. 2002, *A&A*, 395, 1

Fuller, T. M., West, M. J., & Bridges, T. J. 1999, *ApJ*, 519, 22

Hopkins, P. F., Bahcall, N., & Bode, P. 2005, *ApJ* in press

Jing, Y. P. & Suto, Y. 1998, *ApJ*, 503, L9

Jing, Y. P. & Suto, Y. 2000, *ApJ*, 529, L69

Kim, R. S. J., Annis, J., Strauss, M. A., Lupton, R. H., Bahcall, N. A., Cunn, J. E., Kepner, J. V., & Postman, M. 2002, *ASP Conf.Ser.* 268, 393

Klypin, A., Gottlöber, S., Kravtsov, A. V., & Khokhlov, A. M. 1999, *ApJ*, 516, 530

Lee, J. & Pen, U. L. 2000, *ApJ*, 532, 5

Lee, J. & Pen, U. L. 2001, *ApJ*, 555, 106

Lee, J. & Pen, U. L. 2002, *ApJ*, 567, L111

Lee, J. 2004, *ApJ*, 614, L1

Pen, U. L., Lee, J., & Seljak, U. 2000, *ApJ*, 543, L107

Pereira, M. J., & Kuhn, J. R. 2004, preprint [astro-ph/0411710]

Plionis, M., Barrow, J. D., & Frenk, C. S. 1991, *MNRAS*, 249, 662

Plionis, M. 1994, *ApJS*, 95, 401

Plionis, M., & Basilakos, S. 2002, *MNRAS*, 329, L47

Plionis, M., Benoist, C., & Maurogordato, S., Ferrai, C., Basilakos, S. 2003, *ApJ*, 594, 153

Porciani, C., Dekel, A., & Hoffman, Y. 2002, *MNRAS*, 332, 325

Quinn, T., & Binney, J. 1992, *MNRAS*, 255, 729

Rhee, G. F. R. N., & Katgert, P. 1987, *A&A*, 183, 217

Sastry, G. N. 1968, *PASP*, 83, 313

Springel, V., White, S. D. M., Tormen, G., Kauffmann, G. 2001, *MNRAS*, 328, 726

Struble, M. F., & Peebles, P. J. E. 1985, *AJ*, 99, 743

van Haarlem, M., & van de Weygaert, R. 1993, *ApJ*, 418, 544

van Kampen, E., & Rhee, G. F. R. N. 1990, *A&A*, 237, 283

Warren, M. S., Quinn, P. J., Salmon, J. K., & Zurek, W. H. 1992, *ApJ*, 399, 405

West, M. J. 1989, *ApJ*, 347, 610

West, M. J. 1994, *MNRAS*, 268, 79

West, M. J., Villumsen, C., & Dekel, A. 1991, *ApJ*, 369, 287

West, M. J., Jones, C., & Forman, W. 1995, *ApJ*, 451, L5

Zel'dovich, Y. B. 1970, *A& A*, 5, 84

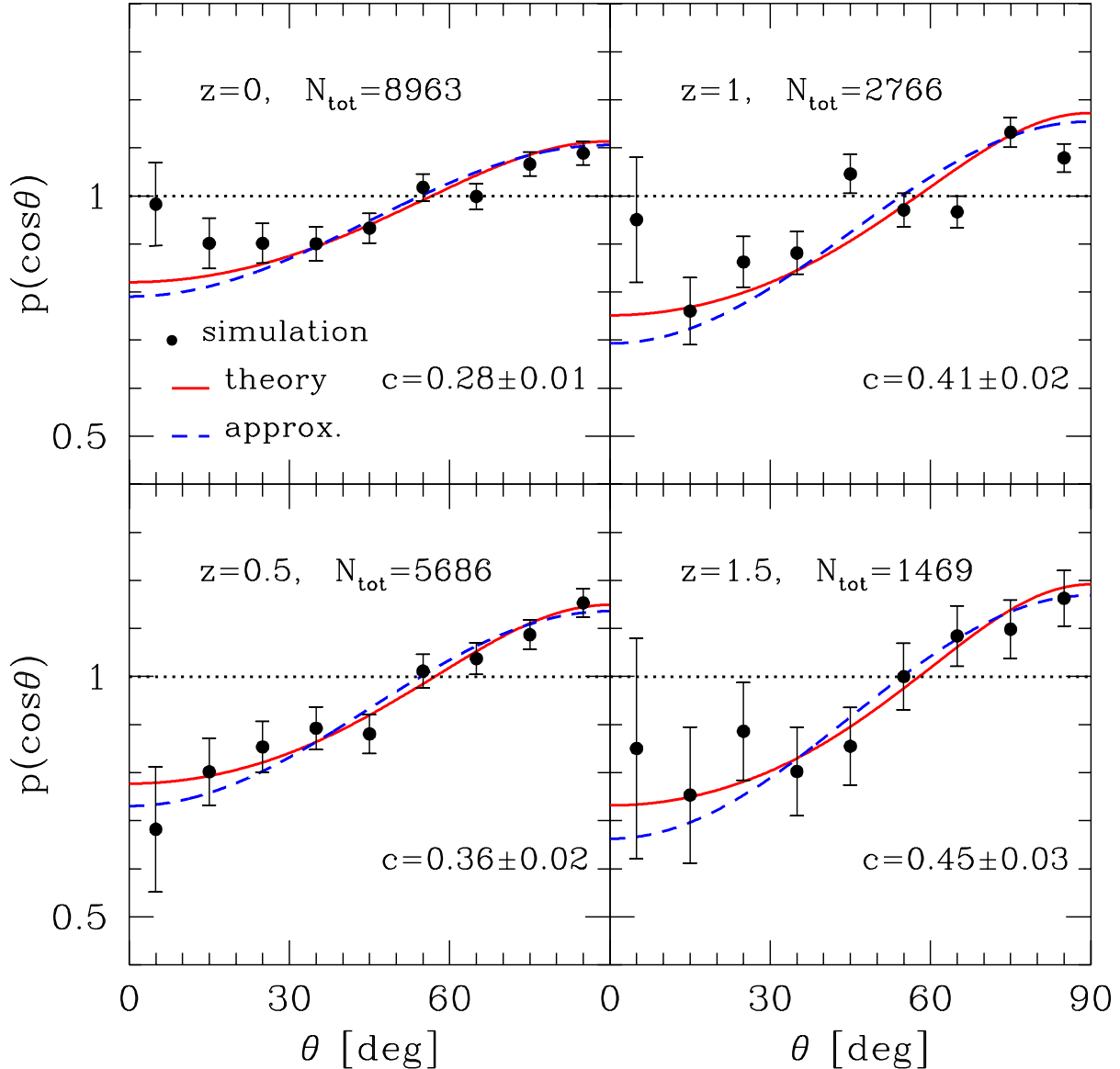


Fig. 1.— Probability density distributions of the angles between the minor axes of the subhalo and the host halo at four different epochs ; $z = 0, 0.5, 1$ and 1.5 . In each panel, the dots represent the simulation results with the Poisson errors, while the solid and dashed lines represent the theoretical prediction (4) and the approximation formula (5), respectively. The horizontal dotted line corresponds to the case of no alignment effect.

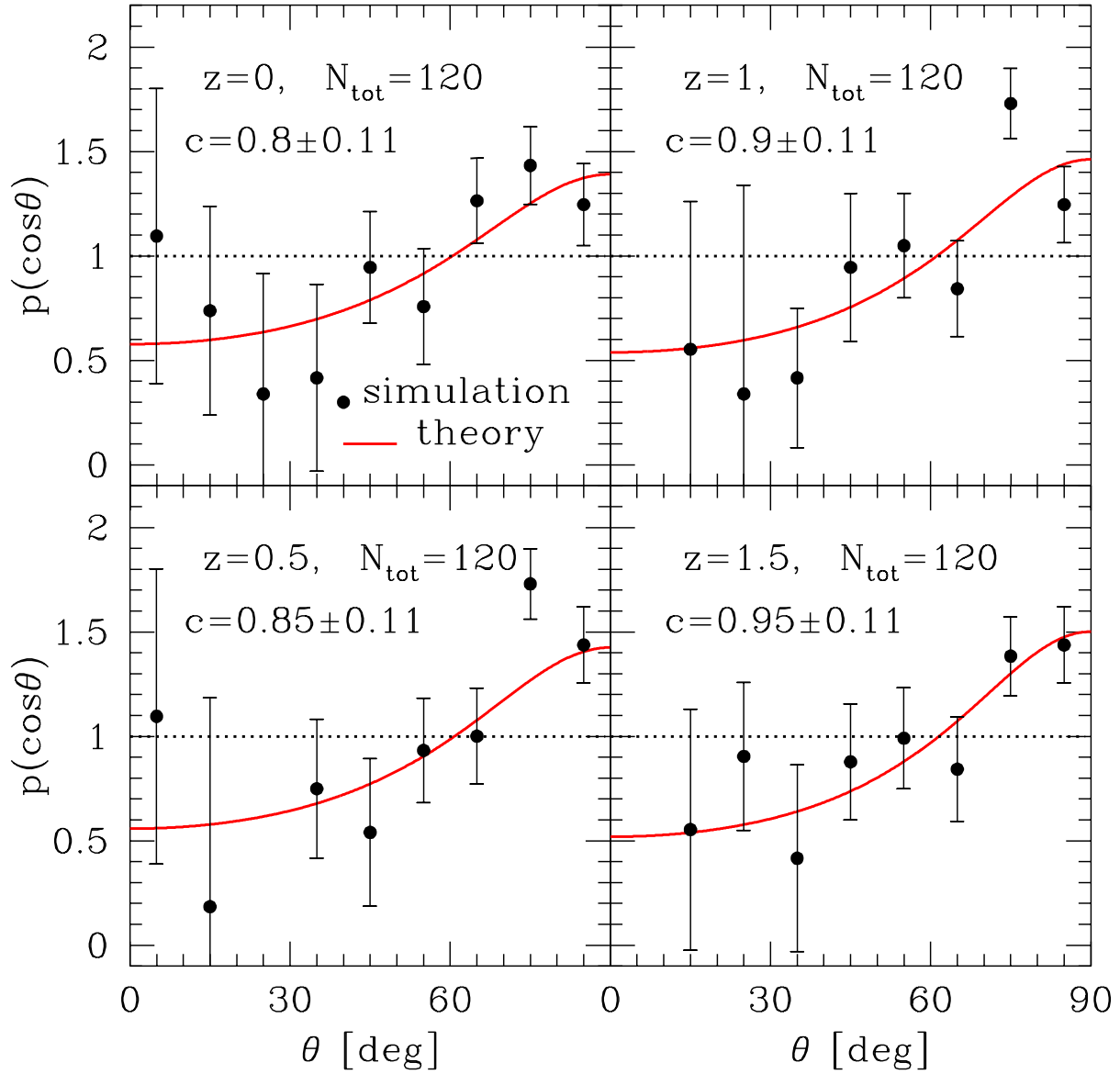


Fig. 2.— Same as figure 1 but with the most massive 30 subhalos.